## SPECIAL ISSUE – NAVY OPERATIONAL MODELS: TEN YEARS LATER

# Navy Sea Ice Prediction Systems

*Ruth H. Preller, Pamela G. Posey*
*Naval Research Laboratory • Stennis Space Center, Mississippi  USA*

*Wieslaw Maslowski, Donald Stark*
*Naval Postgraduate School • Monterey, California  USA*

*Thomas Thang C. Pham*
*Fleet Numerical Meteorology and Oceanography Center • Monterey, California  USA*

The availability of real-time information on sea ice conditions in ice covered seas has always been important, not only to strategic military operations, but to the economies of those countries that border the Arctic and its marginal seas. Knowledge of the thickness and movement of sea ice as well as the locations of open water is required for traversing the Arctic whether in a drill ship, in a cargo vessel or in an ice strengthened ship such as a Coast Guard ice breaker.

Forecasting these conditions is a difficult task at best. The ice and snow that cover the cold Arctic Ocean are highly variable on short time scales, such as days to weeks, and longer time scales of years to decades. This variability in the sea ice cover is due to a combination of dynamic and thermodynamic effects. Surface stresses on the top and bottom of the ice cause the movement of sea ice, or ice drift, as well as the deformation of the ice. Heating and cooling from the atmosphere and the ocean are largely responsible for the growth and decay of sea ice, in combination with the ice motion.

Sea ice has a strong seasonal variability. The thinnest sea ice and largest amount of open water appear in the summer months from June to September. Ice begins to grow back in the fall and builds to a maximum thickness in the late winter and early spring, March-April. Many of the marginal seas, such as the Barents and Greenland Seas are nearly ice free in the summer.

Other marginal seas like the Bering Sea and the Sea of Okhotsk are completely ice free in the summer. These seasonal patterns vary inter-annually as well. This variability is often represented by a seesaw effect when one part of the Arctic experiences a "mild" ice year while another part of the Arctic has an increase in ice extent and/or ice thickness. A general trend overlying this inter-annual variability has been seen by several scientists who have examined long records of satellite data. The trend is for an overall decrease in ice extent from the late 1970s through the mid-1990s (Parkinson et al., 1999; Cavalieri et al., 1997; Johannessen et al., 1995). Whether or not this decrease will continue and what effect it may have on Arctic economics, operations and climatic change is a topic of great international interest.

Sea ice forecasts usually focus on short time scales of 5–7 days. In order to provide an accurate prediction, forecast systems are most often based on a combination of models and data. Modeling sea ice can be a difficult problem, as it exists in many different forms (Figure 1).

It can appear as a field of disjointed ice floes, as a level, continuous field of ice or as a landscape of ice hills and ridges. Interfacial stresses, from the atmosphere and the ocean, interacting with natural coastal boundaries cause the ice to be in a nearly constant state of motion and deformation resulting in the formation of ice rubble, ridges, leads and ice floes. Most sea ice models make the assumption that ice exists as a "continuum". The ice is modeled as having some combination of viscous, plastic, or elastic material characteristics. The way that the ice behaves as a material when acted upon by stress is called ice rheology. Ice within a model grid cell is defined as having a certain thickness and coverage, also defined as a percent of ice concentration. Thickness and concentration are allowed to vary in time depending upon the atmospheric and oceanographic conditions.

The Arctic presents a hostile environment for those trying to gather data on the atmosphere, ice or ocean.

> *Modeling sea ice can be a difficult problem, as it exists in many different forms.*
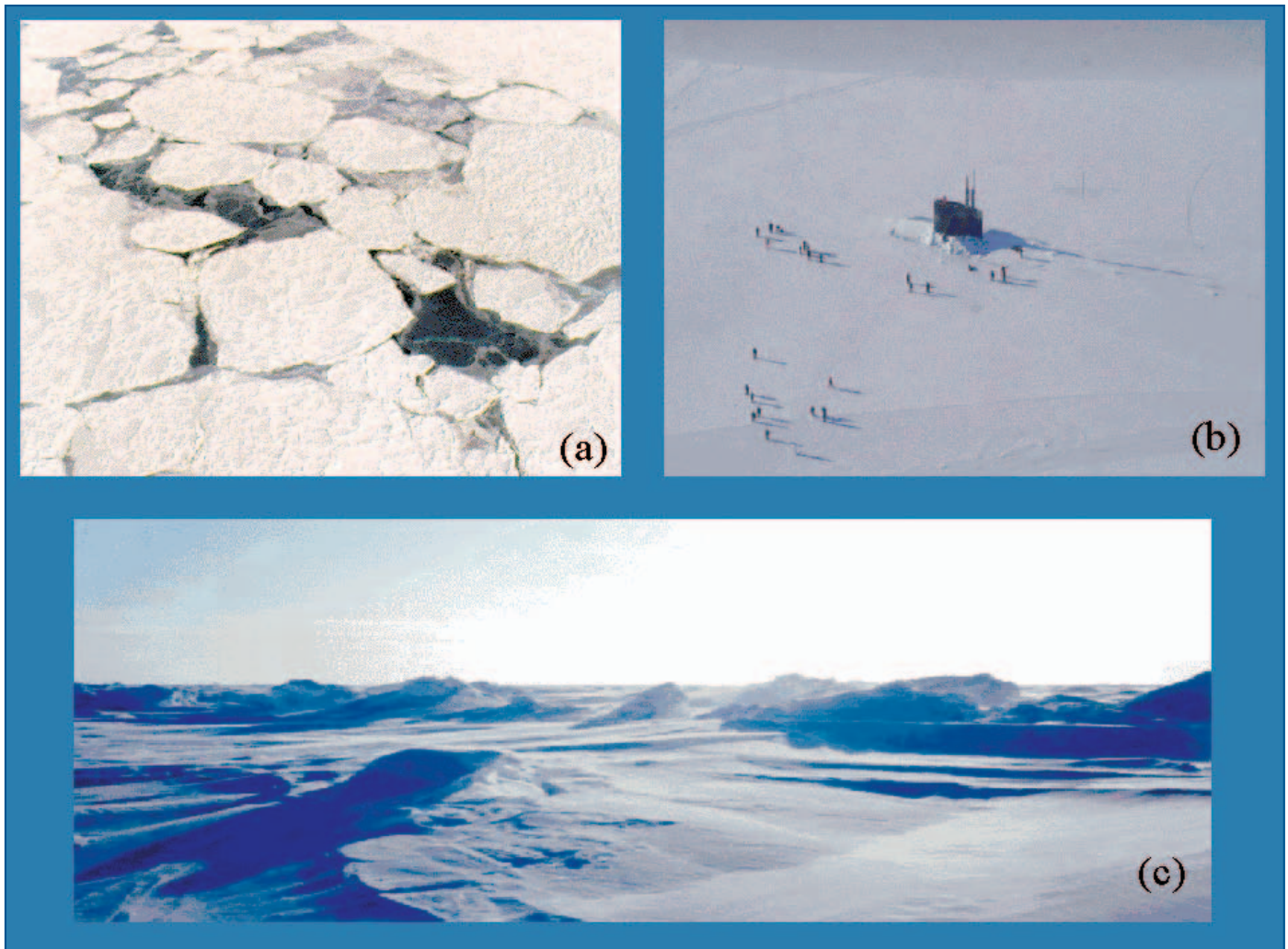
**Figure 1.** *Different forms of sea ice: **a)** ice floes, **b)** a level field of solid sea ice penetrated by the sail of the submarine USS Hawkbill, SCICEX '99 and **c)** ridged ice. Figures are courtesy of **a)** the Canadian Ice Services, **b)** the Arctic Submarine Laboratory and **c)** Ms. Sigrid Salo of NOAA.*

Sub-zero temperatures, strong winds, limited daylight and some intimidating wildlife (Figure 2) make field-work in the Arctic a difficult task.

A majority of observations of the Arctic ice cover, both in real-time and over periods of decades, have been provided by satellite imagery and drifting buoys. Satellite data derived from the Defense Meteorological Satellite Program (DMSP) Operational Line-Scan (OLS) Sensor, the National Oceanic and Atmospheric Administration (NOAA) Advanced Very High Resolution Radiometer (AVHRR), the DMSP Special Sensor Microwave/Imager (SSM/I), and the Canadian RADARSAT are used by forecasting centers like the U.S. Navy/NOAA National Ice Center (NIC) to provide a real-time picture of conditions in the Arctic. A network of automatic drifting data buoys monitoring surface air temperature, pressure and ice motion, has existed in the Arctic basin since early 1979, first under the Arctic Ocean Buoy Program and then in 1991, as part of the International Arctic Buoy Program (IABP). These data have been used to support real-time operations in the Arctic as well as meteorological and oceanographic research of the Arctic basin. More information on the IABP is available at http://iabp.apl. washington.edu/.

Forecasts of ice conditions are produced by numerical ice-ocean models that use these observations to help specify an "initial" state and then run forward in time. The length of the ice forecasts depends on the atmospheric forcing that drives the model. Usually, the forcing is derived from an atmospheric forecast model, and extends about seven days into the future. Longer forecasts (to 30 days) are sometimes generated using persistent atmospheric conditions. The main forecast products that describe sea ice conditions are ice thickness, ice concentration, and ice drift.

Real-time sea ice observations, analyses and forecasts are now available from ice centers around the

**Figure 2.** *Polar bears inspecting a buoy from the International Arctic Buoy Program. This buoy ceased reporting temperatures shortly after this picture was taken. Photo courtesy of D.G. Barton, US Coast Guard (retired).*

world (i.e. Canadian, Swedish, Danish, Japanese, Icelandic centers). These centers are usually responsible for providing information on ice conditions closest to their own coastlines. The U.S. NIC is actively providing global sea ice information to Navy fleet operators and commercial users. In addition to satellite observations, aerial ice reconnaissance, ship/shore station observations, drifting buoy reports, meteorological guidance products, climatology and information from international partners, the NIC uses the forecasts from the Navy's sea ice forecasting system, the Polar Ice Prediction System (PIPS) version 2.0 to generate analyses and forecasts of sea ice conditions in the Arctic.

## The Polar Ice Prediction System (PIPS)

Since the late 1980s, the Naval Research Laboratory (NRL) has been developing sea ice forecast systems for operational use by the U.S. Navy. These models run operationally on computer systems at the Fleet Numerical Meteorology and Oceanography Center (FNMOC). Products are disseminated by FNMOC for use at the NIC. There have been several versions of the Polar Ice Prediction System in the past that have led up to the present PIPS 2.0. The first version of PIPS (PIPS 1.0), operational in 1987, covered the Arctic basin, Barents and Greenland Seas using a horizontal grid resolution of 127 km. PIPS 1.0 was followed by two higher resolution regional models for the Barents Sea, the
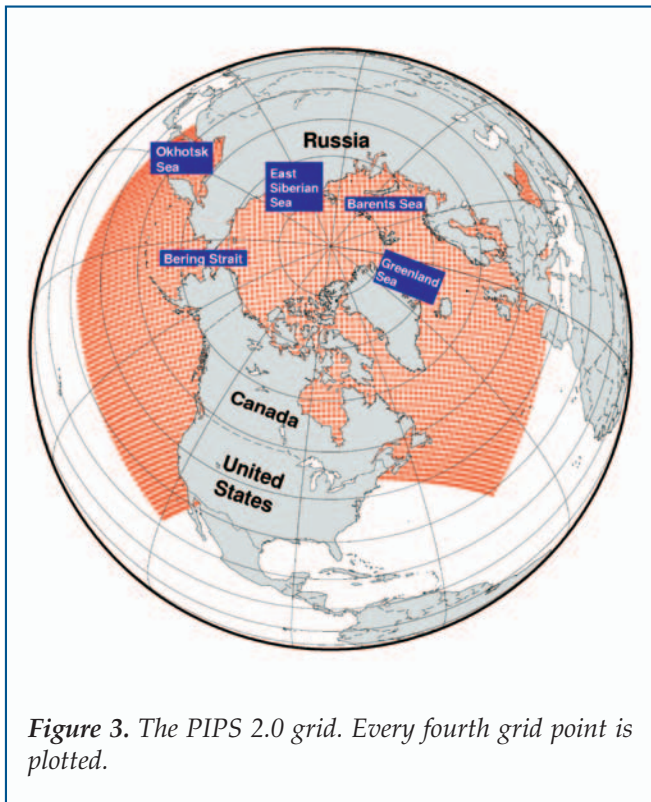
**Figure 3.** *The PIPS 2.0 grid. Every fourth grid point is plotted.*

Regional Polar Ice Prediction System—Barents (RPIPS-B) and for the Greenland Sea, the Regional Polar Ice Prediction System—Greenland Sea (RPIPS-G). The regional models differed from the PIPS 1.0 model in that they covered a smaller area and used higher grid resolution (25 km vs. 127 km). The higher resolution was necessary to provide a better estimate of ice edge and coastlines. These forecast systems made use of an ocean climatology to provide ocean stresses and heat fluxes to the ice model. Atmospheric stresses and fluxes were provided to the ice model by the Navy Operational Global Atmospheric Prediction System (NOGAPS; see Rosmond et al. in this issue). Once these forecast systems were in place, additional requirements were identified. High-resolution forecasts were needed in all of the ice-covered regions of the Northern Hemisphere and sea ice models required coupling to an ocean model to provide daily ocean variability. In response to these requirements, NRL developed the Polar Ice Prediction System 2.0 (PIPS 2.0). This system became operational in 1996 and replaced PIPS 1.0, RPIPS-B and RPIPS-G.

The core of the PIPS 2.0 is a coupled ice-ocean model that consists of the Hibler ice model (Hibler, 1979; 1980) and the Bryan and Cox ocean model (Cox, 1984). PIPS 2.0 coverage extends from the North Pole south, to approximately 30°N latitude and includes marginal seas such as the Sea of Okhotsk, the Sea of Japan and the Yellow Sea in the Pacific and the Gulf of St. Lawrence and the Labrador Sea in the Atlantic (Cheng and Preller, 1996). The grid resolution, 0.28°,

varies from 17–33 km depending on the location of the grid square within the spherical coordinate system (Figure 3). PIPS 2.0 uses a rotated coordinate system to avoid the problem of a numerical singularity at the pole.

For both the ice and ocean models, the lateral boundaries are defined as solid walls and placed away from any sea ice covered regions in order to minimize their effect on sea ice forecast areas of interest. Following the technique of Sarmiento and Bryan (1982), the ocean model temperature and salinity fields are loosely constrained to the Levitus (1982) climatological data set using a 250 day restoring time at all levels of the ocean. This weak constraint on the ocean temperature and salinity does not adversely affect the PIPS 2.0 ability to forecast ocean variability on the daily to weekly time scales. The bathymetry used by the ocean model is derived from a U.S. Navy 5 minute data base called the Navy Digital Bathymetry Data Base 5' x 5' (DBDBV; NAVOCEANO, 1997).

In this coupled system, the ocean model provides input to the ice model in terms of ocean currents, salinity and heat fluxes (temperatures). The ice model provides salinity and temperature changes due to the growth and decay of sea ice and surface stresses to the ocean model. The ocean model contains 15 vertical levels, each level increasing in thickness with depth. Direct interaction between the ice and ocean model occurs in the first level that is 30 m deep and represents the ocean mixed layer.

Figure 4 is a schematic of the design of PIPS 2.0. At the center of the system, is the coupled Hibler ice model/Cox ocean model. Atmospheric forcing is provided by NOGAPS. The atmospheric forcing fields used by the forecast system are surface wind stress, surface air temperature, surface pressure, surface vapor pressure, shortwave radiation, sensible plus latent heat flux, and the total heat flux. The system produces a 120-hour forecast each day. In addition to the output of the model (ice drift, thickness, concentration, growth/decay of ice, ocean currents, temperature and salinity), restart fields consisting of the model's 24-hour forecast are written to a file to be used to initialize the next day's forecast. If the model restart fields are not available, a model-derived climatology is used to initialize the forecast.

The quality of each forecast depends strongly on the accuracy of the initial conditions and the atmospheric forecasts, as well as on the inherent accuracy of the forecast model. If the unaltered 24-hour forecast is used to initialize the forecast, these errors will inevitably compound eventually leading to unacceptably large forecast errors. To reduce this effect, the 24-hour forecast fields are used in combination with observed ice concentration data to initialize the model. The PIPS 2.0 assimilates ice concentration data from the DMSP Special Sensor Microwave/Imager (SSM/I). These data are chosen for three reasons: they are available daily, in real time, at FNMOC; the resolution of the data is similar to the resolution of the model; and the
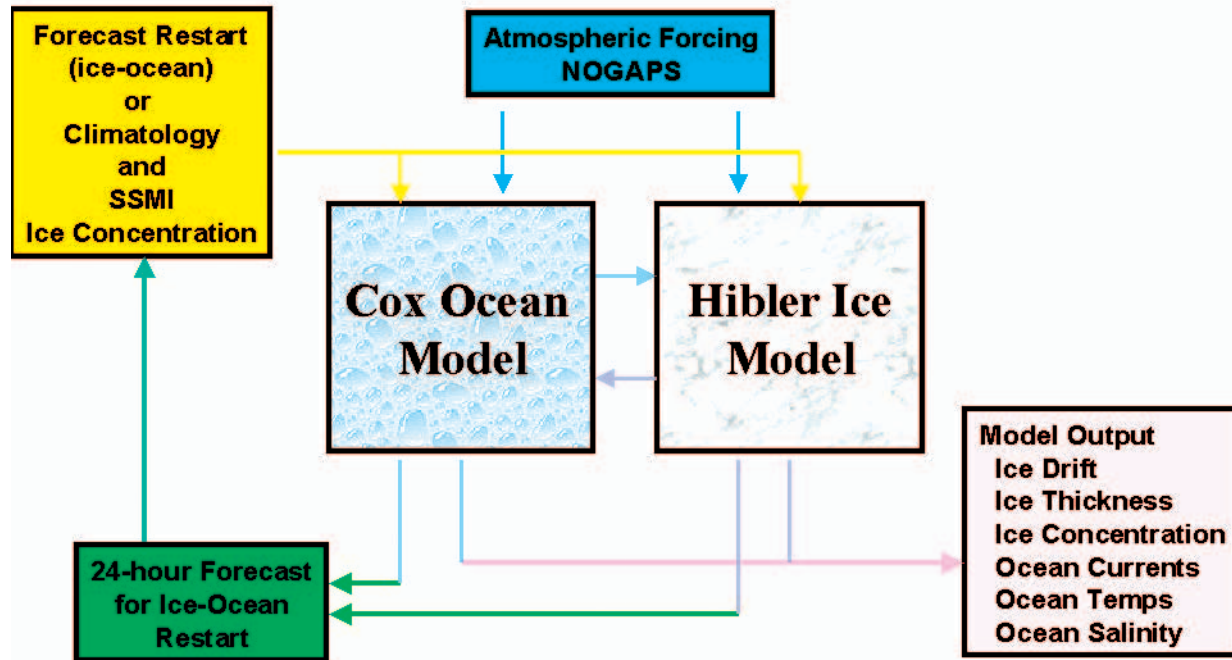
## Polar Ice Prediction System 2.0



**Figure 4.** *A schematic of the PIPS 2.0 sea ice forecasting system.*

data cover the entire model domain. The SSM/I brightness temperatures are converted into ice concentration data using the Navy CAL/VAL algorithm (Hollinger et al., 1991) at FNMOC. This algorithm is sensitive to the ice/water boundary and to thin ice. As such it provides a good estimate of the location of the ice edge and a better estimate of thin ice than most other algorithms. However, due to its sensitivity to thin ice, it often saturates too quickly to 100% ice concentration, producing an overestimate of high ice concentrations. For more information on algorithm descriptions and comparisons see http://www.natice.noaa.gov/science/products/descriptions.html.

After the PIPS 2.0 restart fields are read into the model, the daily SSM/I ice concentration data, interpolated to the model grid, are read in. Based on the characteristics of the CAL/VAL algorithm, the SSM/I data replaces the model-derived ice concentration only at locations where observed concentration is greater than 80% or less than 50% and, the difference between the two fields is greater than 10% or 5% respectively. The model-derived ice thickness field and the ocean surface temperature field are then adjusted to be consistent with the concentration data. That is, if the

SSM/I data indicate there is no ice where the model had produced ice, ice is removed from the model field and the ocean temperature is raised one degree above freezing to restrict immediate ice growth in this location. If the model did not have ice in a location where the SSM/I sees ice, a small amount of ice (0.3–0.6 m) is added to the model thickness field and the ocean temperature is set to the freezing temperature of sea ice. These adjustment values were determined from a series of model experiments. As the adjustments are usually confined to a few grid cells near the ice edge, the experiments showed no serious dynamical/numerical problems associated with the technique.

## Forecast Products

Since the end of July 1996, PIPS 2.0 has been producing operational 120-hour forecasts daily. Each day a set of 11 products is generated from the PIPS 2.0 forecast (Table 1). These products, and the interval at which they are generated, are determined by the NIC. They are transmitted to the NIC in GRIB format and may be viewed as a graphic product on NIC workstations. The NIC uses PIPS 2.0 products as guidance in generating their ice analysis and forecast products.

## Table 1
### PIPS 2.0 Daily Operational Products

| Product | Depth*(m) | Forecast Time (hrs) |
|---|---|---|
| Ice Thickness | — | 0, 24, 48, 72, 96, 120 |
| Ice Concentration | — | 0, 24, 48, 72, 96, 120 |
| Ice Drift | — | 6, 12, 18, 24, 48, 72, 96, 120 |
| Divergence/Convergence | — | 6, 12, 18, 24, 48, 72, 96, 120 |
| Ocean Currents | 15.0 | 6, 12, 18, 24, 48, 72, 96, 120 |
| | 53.0 | 6, 12, 18, 24, 48, 72, 96, 120 |
| | 110.0 | 6, 12, 18, 24, 48, 72, 96, 120 |
| Ocean Temperature | 15.0 | 24, 48, 72, 96, 120 |
| | 53.0 | 24, 48, 72, 96, 120 |
| | 110.0 | 24, 48, 72, 96, 120 |
| Ocean Salinity | 15.0 | 24, 48, 72, 96, 120 |

*Depth is at the center of each level

Figures 5b–d are examples of standard products from the system: ice displacement (based on the ice drift), ice concentration and ice thickness. Figure 5a represents the observed ice motion derived from the available IABP drifting buoys. Figures 5a and 5b show the qualitative similarities between the PIPS 2.0 forecast and the observed ice motion. PIPS 2.0 also has the capability to forecast ocean currents, ocean temperature and salinity. Recently these fields were requested by the NIC as input to a marginal ice zone specific ice model that is being developed and tested for the center's use.

## Future Sea Ice Forecast Systems—PIPS 3.0

In the pre-operational evaluation of PIPS 2.0 products (Preller and Posey, 1995) the original PIPS and PIPS 2.0 ice drift were evaluated against Arctic buoy data. These results showed that PIPS 2.0 produced an improved ice drift forecast over PIPS with a decrease in the Root Mean Squared (RMS) Error of about 10–15%. Due to the combination of the increased resolution and the incorporation of an ocean model versus an ocean climatology, the PIPS 2.0 ice edge was a substantial improvement over the existing PIPS models, including the higher resolution regional models.

A recent study by a group of scientists from the NIC and NOAA (Van Woert et al., 2001), showed that although the PIPS 2.0 forecasts (48-hour) were better than persistence on average, there were still substantial biases in its prediction of the growth and decay of sea ice in the marginal ice zone. PIPS 2.0 often over-predicts the amount of ice in the Barents Sea and therefore often places the ice edge too far south. In contrast, PIPS 2.0 often under-predicts the ice extent in the Labrador Sea and Hudson Bay. As forecasts are a combination of many different components (Figure 4)—atmospheric forcing, oceanographic forcing, model parameterizations and initialization—the combination of even small errors from each of these pieces could add up to a substantial error in the forecast.

In recent years, there has been a request for the capability to predict the location of regions of open water within the ice pack. Approximately 1% of the central Arctic ice pack is estimated to be open water in winter. In summer, the amount increases to 10–20% (Gow and Tucker, 1990). Openings in the ice pack usually appear in two forms: leads and polynyas. Leads are crack-like openings in the ice pack, usually tens to hundreds of meters wide, while polynyas are larger, more permanent openings. Leads form in regions where large-scale divergent wind patterns produce divergent stresses in the ice causing the ice to break apart. Leads appear as linear features in compact ice that often have a preferential orientation (direction). Polynyas form near coastlines where divergence or shearing of the pack ice separates the ice from the coast or from a fast ice boundary. Leads and polynyas are significant because they provide traversable areas in the ice pack for ships. In addition they are important because they are regions of very large heat-loss to the atmosphere. Winter leads rapidly refreeze, due to the heat loss to the atmosphere, forming young thin ice that is easily deformed. Leads and polynyas are a major source of new ice growth in winter. Although PIPS 2.0 can predict large-scale polynyas, it does not have the capability to produce smaller polynyas or leads or to provide guidance on lead orientation.

PIPS 2.0 is based on the scientific research efforts of late 1970s and early 1980s. During the past 10 years (1990s), great strides have been made in understanding

sea ice dynamics and thermodynamics as well as observing ice conditions. An additional and very important factor in the improvement of ice modeling and forecast capabilities is the advance in computer technology over the past 10 years. Computer codes now make use of multiple processors and can perform more extensive computations in operationally acceptable time periods.

In 1998, the Office of Naval Research (ONR) and the Oceanographer of the Navy via the Space and Naval Warfare Systems Command (SPAWAR) joined forces to fund an effort to combine this new technology and data into an improved sea ice forecasting system. This system, aptly named PIPS 3.0 (http://www.oc.-nps.navy.mil/~pips3) is presently being developed through a joint effort among the U.S. Naval Postgraduate School, various other academic institutions and the Naval Research Laboratory. The PIPS 3.0 ice model will contain an improved calculation of ice growth/decay based on the use of a multi-level ice
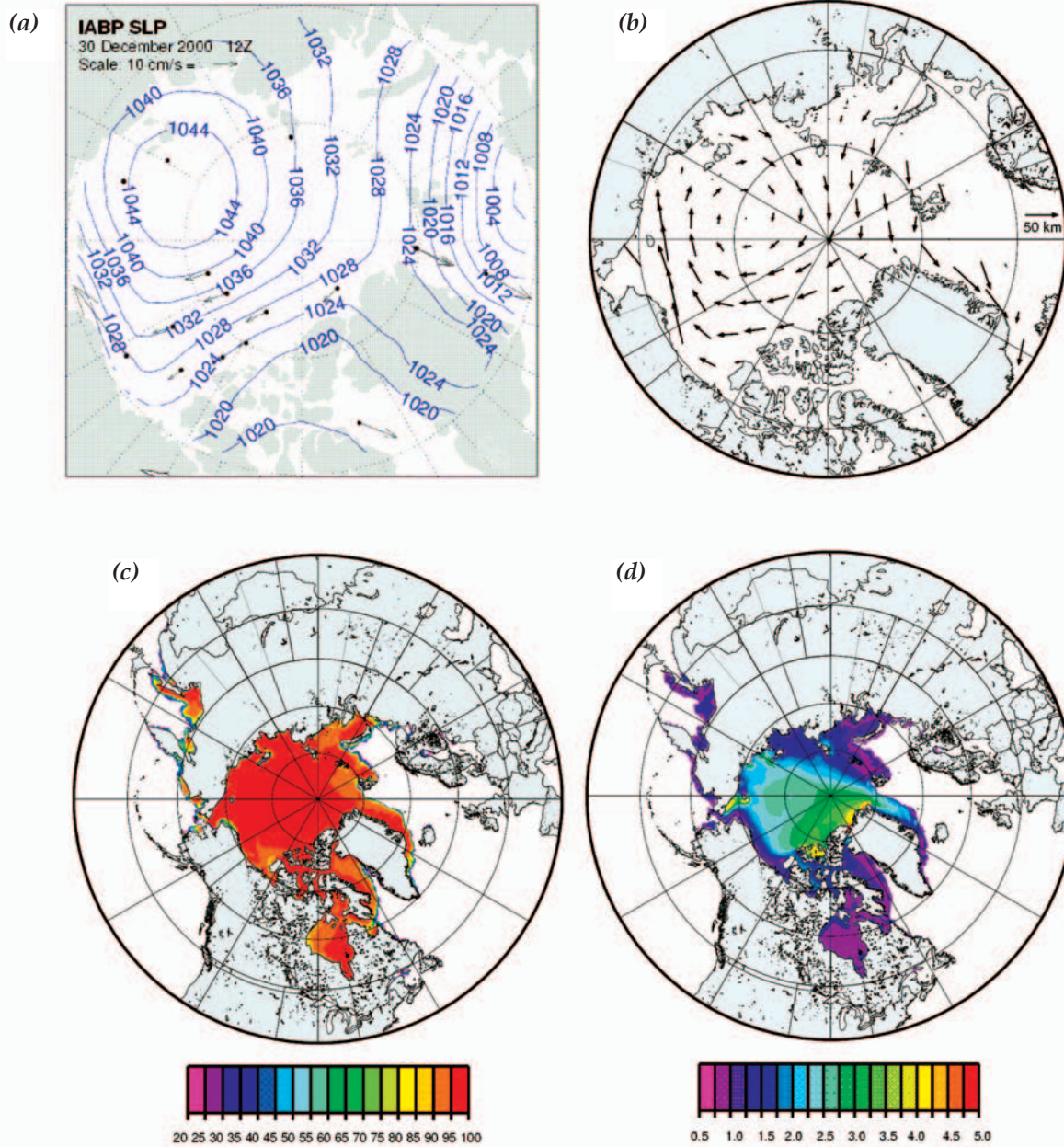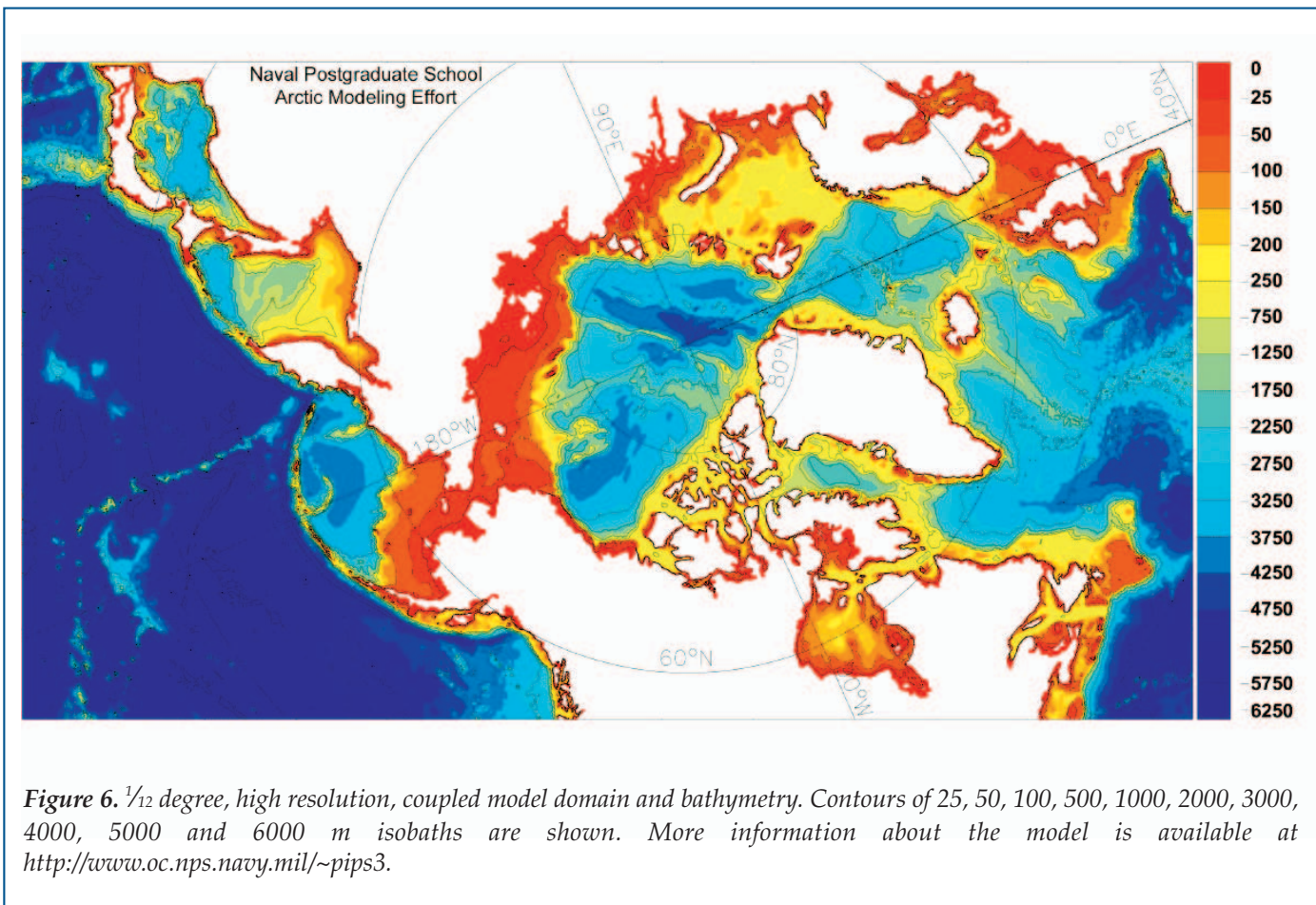


**Figure 5.** *IABP buoy drift and PIPS 2.0 72-hour forecast products from December 30, 2000. **a)** IABP buoy drift in cm/sec and sea level pressure in millibars, **b)** 72-hour ice displacement in kilometers, **c)** ice concentration in percent and **d)** ice thickness in meters.*

**Figure 6.** *¹/₁₂ degree, high resolution, coupled model domain and bathymetry. Contours of 25, 50, 100, 500, 1000, 2000, 3000, 4000, 5000 and 6000 m isobaths are shown. More information about the model is available at http://www.oc.nps.navy.mil/~pips3.*

thickness formulation. Ice edge forecasts will be improved by using higher horizontal resolution. Ice motion and ice edge location will be improved by the assimilation of satellite derived ice drift data. In addition, higher resolution and more realistic ice rheology will improve the PIPS ability to predict areas of lead formation and lead orientation.

These improvements to the PIPS 2.0 are being tested in an incremental fashion. The first tests were designed to examine the effects of higher resolution on an ice model similar to that of PIPS 2.0 coupled to an improved ocean model with improved bathymetry. At the same time, techniques for the assimilation of satellite derived ice drift into the ice model were developed and tested. Results from these tests are described below.

## High Resolution Coupled Model Tests

Similar to the PIPS 2.0, the coupled ice-ocean model used in these experiments extends from the North Pacific (at ~30°N) through the Arctic Ocean and the Nordic Seas into the North Atlantic (to ~45°N; Figure 6) and uses a rotated coordinate system. The ice and ocean model horizontal grid is configured at ¹/₁₂° (~9 km) with 45 vertical levels in the ocean. In the vertical direction, the upper 100 meters of the ocean are

resolved by eleven layers, and the upper 500 meters of the ocean by nineteen layers. This resolution allows detailed representation of bathymetry over the vast Arctic shelves and in marginal seas as well as many local bathymetric features important to large-scale ocean circulation (e.g. St. Anna Trough, Canadian Archipelago, or Bering Strait). The bathymetry data used to define the grid shown in Figure 6 consists of the ETOPO5 database (National Geophysical Data Center, 1988), NRL charts and Canadian Hydrographic Center charts for latitudes south of 64°N. North of 64°N, the 2.5 km resolution International Bathymetric Chart of the Arctic Ocean (IBCAO) database (Jakobsson et al., 2000) is used. These data represent a considerable improvement over previous data available for this area used in PIPS 2.0. This high resolution, coupled ice-ocean model is an extension of previous modeling research using a horizontal resolution of ¹/₆° and 30 vertical levels (Maslowski et al., 2000, 2002; Zhang et al., 1999, http://www.oc.nps.navy.mil/sbi). The coupled model adapts the Los Alamos National Laboratory (LANL) global Parallel Ocean Program (POP) ocean model with a free surface (Maltrud et al., 1998; Dukowicz and Smith, 1994). The sea ice model at present is similar to PIPS 2.0 with a viscous-plastic rheology, the zero-layer approximation of heat conduction

through ice and a surface energy budget calculated following Parkinson and Washington (1979). The main difference between this ice model and the PIPS 2.0 ice model is its ability to utilize modern parallel computer architectures.

A 27-year spin-up integration of the coupled ice-ocean model has been run, forced with a daily-averaged annual cycle of climatological atmospheric fields derived from the European Centre for Medium-range Weather Forecasts (ECMWF) 1979–1993 reanalysis. Forcing fields include: 10-meter winds, surface pressure, surface air temperature and dew point, and long-wave and short-wave radiation. During the spinup, the ocean surface temperature and salinity are restored with a 30-day time scale to monthly mean climatology derived from the University of Washington's Polar Science Center Hydrographic Climatology (PHC; Steele et al., 2001).

Following the 27-year integration, an additional 12-year run has been completed using the repeated 1979 ECMWF annual cycle for the first 6 years and 1979–1981 inter-annual fields for the last 6 years. This approach has been used to force the sea ice and ocean states towards conditions of the late 1970s and early 1980s. These conditions may then be used to initialize the new version of the PIPS 2.0 ice model and spin it up to the present day for forecast use.

Understanding the ice thickness distribution and its variability is important in both short-term operational forecasts and longer-term climate studies. Model-derived ice thickness fields are useful in obtaining a large-scale, but detailed picture of ice distribution and, more importantly, an understanding of its temporal variability.

In Figure 7, the 3-year mean ice thickness distribution is presented from the first three years of the 1979–1981 output. The modeled distribution of ice thickness compares reasonably well to that known from observations (Bourke and Garrett, 1987; Bourke and McClaren, 1992). In agreement with data, the thickest ice (> 6.0 m) in the Arctic is found along the Canadian Archipelago and northern coast of Greenland. Farther north near the pole, the ice thickness decreases to values of 3.0–3.5 m. This simulation also shows relatively thick ice (> 3.5 m) on the East Siberian shelf. Since few observations are available for that region and that time, it is difficult to quantitatively verify these results. In the 1990s, measurements of ice thickness were made in the central Arctic Ocean from U.S. Navy submarines and at a number of key point
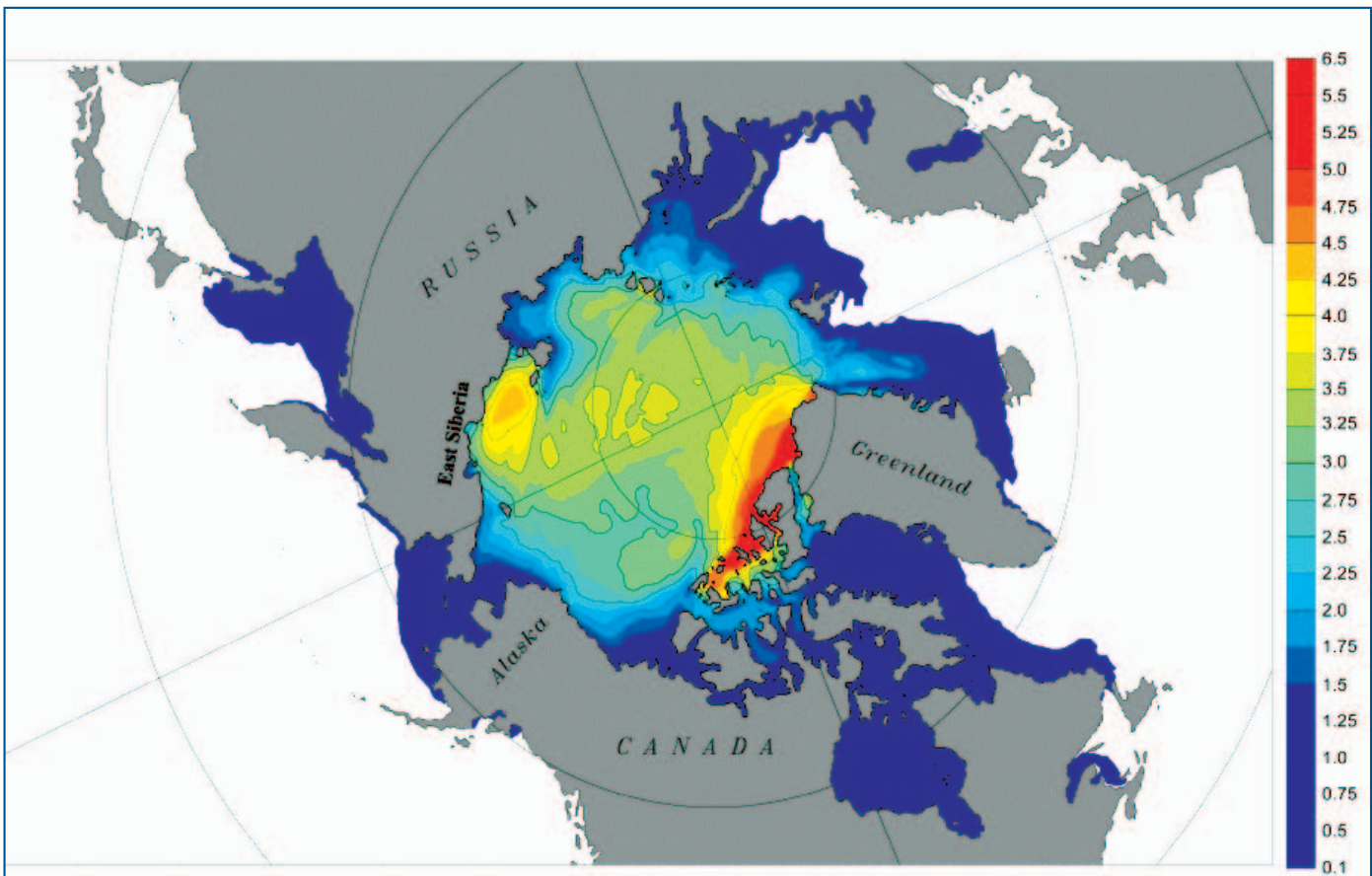


**Figure 7.** *Three-year mean sea ice thickness for 1979–1981. The line-contour interval is 0.5 m.*

locations (e.g. the Fram Strait) using upward looking sonar. Model results will be verified against these recent observations once the model output for that time period becomes available. Based on the comparisons made thus far, these model results look promising in terms of forecasting ice thickness and ice edge variability.

Coupled ice-ocean models, such as those used by PIPS 2.0 and PIPS 3.0, are most often applied in academic studies of global climate issues such as climate change. In these studies the models are used for decadal or longer simulations and focus on long term changes in the overall pattern of ice thickness and ice extent. This application of the coupled model requires access to powerful computers and large quantities of computer time. However, coupled ice-ocean models used for forecasting face a different set of requirements. As forecasts are concerned with sea ice variability on much shorter time scales, the models must be designed to produce the most accurate daily changes in ice concentration, ice edge location and ice motion. These models are required to go through rigorous validation studies to prove their capability to produce accurate short term variability. Data assimilation plays a major role in the accuracy of these forecasts. Once operational, continuous quality control and evaluation of the products may be used to upgrade the system and improve forecast accuracy. In addition, forecast systems are limited by the amount of computer resources available for each forecast as they compete with other forecast models each day. Therefore the combined model/assimilation system must be designed to "fit" within these limitations. This places restrictions on the "size" or grid resolution of the models as well as the complexity of the model parameterizations and the data assimilation techniques. Each of these issues must be taken into account when developing a new forecast system.

## PIPS 3.0 Ice Motion Data Assimilation

As stated earlier, a popular strategy to reduce the initial error in numerical forecast models is to use information from real-time observations to correct the previous forecast field through data assimilation. Data assimilation analysis makes use of a predictor-corrector strategy, where the model predicted ice state (known as the background field) is corrected by whatever observations are available. The specific process of correction fundamentally determines the nature of the assimilation. Current ice state observations tend to be either scattered through space or infrequent in time. They may also contain noise that can introduce non-physical structure into the model. The direct replacement of model values with the observed values (known as insertion) can have undesirable consequences. It is therefore, preferable to employ some sort of self-consistent procedure that reduces the error and distributes the observational knowledge widely

over the domain. Statistical assimilation methods meet these criteria.

One of the first investigations of the assimilation of ice motion data into a stand-alone ice model (similar to the original PIPS 1.0) employs the optimal interpolation methodology (Meier et al., 2000). Optimal interpolation is the simplest type of statistical assimilation. Statistical assimilation means that the background field is corrected to "minimize the error statistics" of the assimilated field. This can be done, only if the error statistics of the observations and the model are known. The technique is "optimal" since the error variance is minimized.

Individual ice velocity vectors of the background field are corrected by applying a linear combination of the nearby observed ice motions. The correction coefficient for each observed value results from solving a linear system dependent, among other things, on the ratio of the model to data error covariances. When these weights are applied to the corresponding observations, the resulting correction minimizes the error variance of the corrected solution. This formula illustrates that it is not sufficient to be concerned with the observed ice motions alone. The error statistics for the model and the data are just as important. They instruct the algorithm as to which observations to use, and what relative weight they must have, in order for the correction to minimize the error.

Two types of ice motion observations are used. The first, which provides the data to be assimilated, is not directly observable. It is derived from the SSM/I passive microwave brightness temperature imagery through a technique known as feature tracking. Individual swaths of the SSM/I satellite are combined or "composited" into a daily gridded field. The displacement of features common to the fields on consecutive days can provide an estimate of the ice velocity. The derived ice motion observations used here were obtained from the Polar Remote Sensing Group at the NASA Jet Propulsion Laboratory (Kwok et al., 1998). They were chosen for the assimilation analysis because they are similar to the real-time ice motion products that will be available from FNMOC. Ice motion observations are available daily from the beginning of October through the end of May. The data are not available for the summer months due to the susceptibility of the passive microwave signal to excessive error from moisture in the form of either heavy summer cloud cover or the formation of melt ponds in the ice.

The second set of observations comes from IABP drifting ice buoys (Rigor and Heiberg, 1997). In the operational configuration of the model, the buoy motions will be included as observations to be assimilated. This will be especially important in the summer months when SSM/I derived motions are not available. The buoys were withheld in this study to be used for validation purposes, and to compute the error covariances. For the period of the study, there are roughly 30 buoys, irregularly distributed throughout the Arctic, at
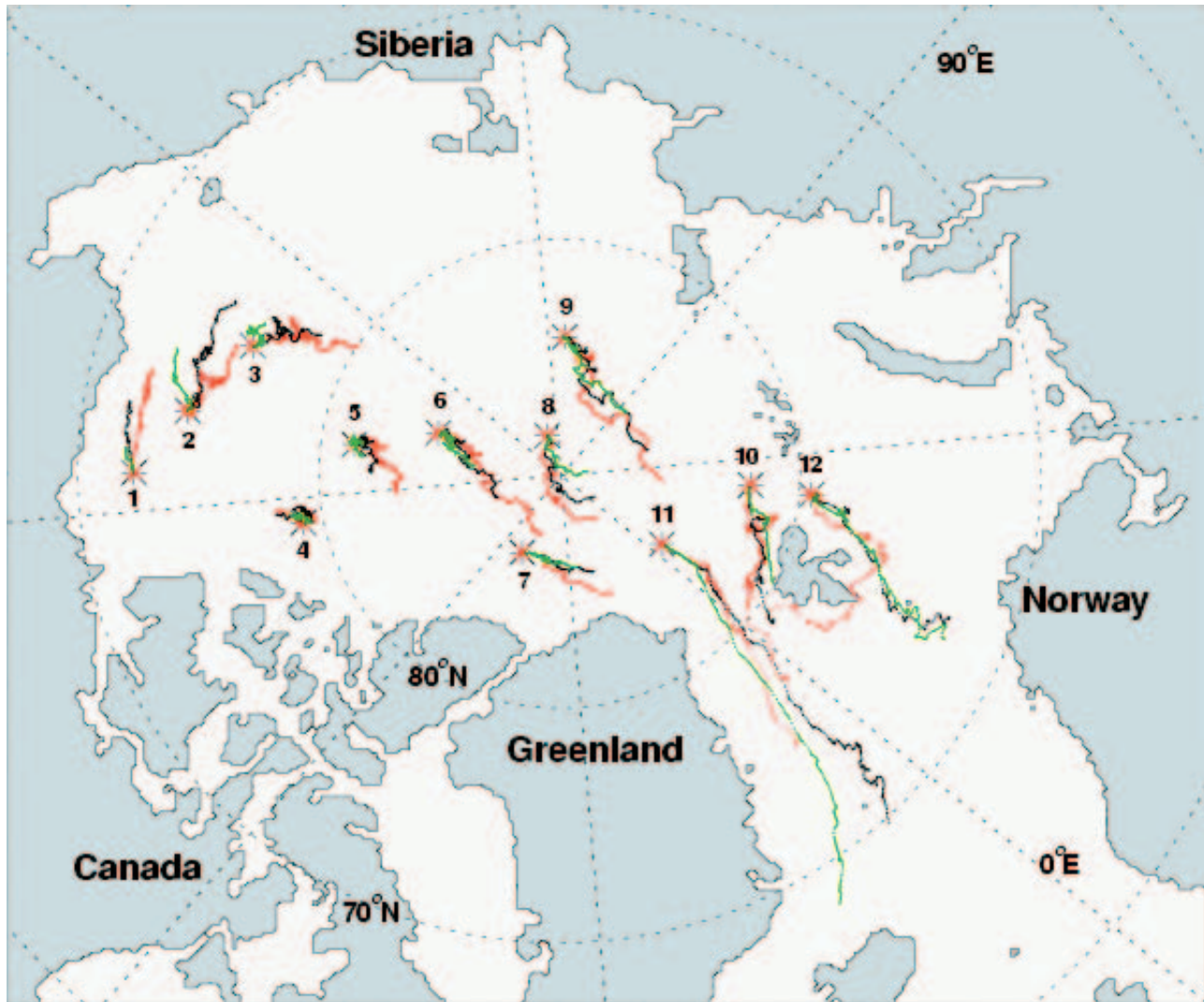
*Figure 8. Ice drift for the IABP drifting buoys (red), the model (green), and the model with assimilation (black).*

any time. Each buoy transmits its location twice per day. The ice buoy velocity can then be calculated from the spatial displacement of the buoy location.

As a test of concept, this proposed PIPS 3.0 ice motion assimilation method was instituted in a previously tested high resolution fully coupled sea-ice/ocean model (Zhang et al., 1999). The coupled sea-ice/ocean model employs a reduced domain consisting of the Arctic basin, with a closed Bering Strait, and extending south into the Atlantic to about 50°N. The spatial resolution of the model is roughly 18 km: half the resolution proposed for the PIPS 3.0 model. The model can be run in either control (no assimilation) or assimilation mode.

Two model runs were generated for the period from January 1992 through December 1994. The ECMWF reanalysis product provided the atmospheric forcing in both configurations. In the control run, no assimilation takes place. In the assimilative run, the model digests the derived SSM/I ice motion product for the months of October through May of each year. During the summer months, no assimilation takes place. The drifting ice buoy data are withheld as validation. Figure 8 shows selected trajectories of the IABP drifting buoys, the control run and the assimilative run. Trajectories from the control run and the assimilative run are produced by integrating forward in time from the initial buoy location using a standard fourth-order Runge-Kutta method and the respective daily instantaneous velocity field. The trajectories displayed represent the range of ice motion behavior seen during the spring of 1992, and the period covering the fall of 1992 through the spring of 1993. The subset of trajectories displayed in the figure was chosen for its coverage of

the figure domain. The trajectories for the control run and the assimilative run have the same starting locations, and the same starting and ending dates as the buoys.

Consider the trajectories numbered 1–10. Both the control run (green) and the assimilative run (black) generated motions are consistently slower than the buoy motion (red). The pattern of buoy twists and turns is strongly reflected in the assimilative run trajectories for about a half of the cases. The error, for the assimilative run trajectories, is largely due to the difference in speed. The error in the control run is manifested in terms of an even greater speed differential as well as large errors in the direction of the motion. In nine out of the ten cases, the assimilative run produces a trajectory that more closely follows the buoy trajectory then does the control run's trajectory. The assimilation process generally increases the ice speed, and preserves the observed direction of the ice motion. On average, the trajectories with assimilation contain half the error of the trajectories without assimilation.

The remaining two trajectories (11 and 12) illustrate a different situation. The marginal ice zone (MIZ) in the Greenland Sea is extremely dynamic, commonly exhibiting the largest ice speeds of anywhere in the domain. In addition, south of 80°N there are very few SSM/I derived observations that can be assimilated, and those that exist tend to have large error bounds. As a result, trajectories south of 80°N can have quite large errors. For trajectory 12, which starts east of Spitsbergen, the buoy moves clockwise, encircling the island. In contrast, the trajectories representing the control run and the assimilative run speed south into the Norwegian Sea. The similarity between these two trajectories is due to the lack of SSM/I derived ice motions to assimilate. The difference in the path of the two trajectories reflects the difference between the ice states for that location in the two model runs. Since the current ice state for a given location is a function of its history, each model can have ice with different concentration and thickness characteristics. The different ice characteristics can result in different reactions to the same forcing.

Trajectory 11 shows the buoy flowing south into the Fram Strait and along eastern Greenland. Initially, the three trajectories are indistinguishable. As they approach Fram Strait, the trajectory from the control run begins to diverge from the path of the other two. From the starting location to approximately 79°N, the assimilative run produces a trajectory that coincides well with the buoy. Past this point, where there are no longer any SSM/I derived motions for the model to assimilate, the three trajectories rapidly diverge. Eventually, both the control run and the assimilative run produce trajectories that travel up to twice as far as the buoy, with the control run's trajectory traveling the farthest. Neither of the model runs, with or without data assimilation, realistically represents the buoy motion south of the Fram Strait. These two cases illustrate the need for the assimilation of the buoy motions in regions where the SSM/I derived motions are not available. In addition, the buoy tracks can provide badly needed data during the summer season, when SSM/I derived products are not available. Further details on the assimilative model can be found in Stark (2001).

## Summary

The U.S. Navy has been running sea ice forecast systems operationally since the late 1980s. These models have been gradually upgraded through the years to higher resolution, data assimilative models that span more of the sea ice covered oceans in the Northern Hemisphere.

The models have provided forecasts of ice motion, ice thickness and ice coverage over regions that are physically difficult to observe due to hostile environmental conditions. Advancements in satellite technology provide these forecast systems with continuously improving data for assimilation, thus enabling improvements to the daily forecasts. Advancements in computer technology provide these forecast systems larger and faster computers to generate improved forecasts.

The most recent upgrade to the Navy's ice prediction capability is the development of the next generation forecast system, PIPS 3.0. Improvements to this new forecast system include, higher horizontal resolution, a more sophisticated ocean model, improved data assimilation and perhaps most important, an improved sea ice model. The ongoing upgrade of the sea ice model will include a Lagrangian formulation for calculating a multi-category ice thickness distribution, a snow layer, a brine pocket parameterization, non-linear profiles of temperature and salinity (Bitz and Lipscomb, 1999), and a Coulombic yield curve for the viscous-plastic rheology (Hibler, 2000). These improvements are geared towards providing better forecasts of ice edge, ice motion, ice thickness and regions of lead formation and lead orientation. The PIPS 3.0 is presently going through its final development and will begin its adaptation for operational use next year with a scheduled transition into operational use in late 2002 or early 2003.

## Acknowledgements

# References

Bitz, C.M. and W.H. Lipscomb, 1999: An energy conserving thermodynamic model of sea ice. *J. Geophys. Res.*, 104(C7), 15669–15677.

Bourke, R.H. and R.P. Garrett, 1987: Sea ice thickness distribution in the Arctic Ocean. *Cold Reg. Sci. Technol.*, 13, 259–280.

Bourke, R.H. and A.S. McClaren, 1992: Contour mapping of Arctic basin ice draft and roughness parameters. *J. Geophys. Res.*, 97(C11), 17715–17728.

Cavalieri, D.J., P. Gloersen, C.L. Parkinson, J.C. Comiso and H.J. Zwally, 1997: Observed hemispheric asymmetry in global sea ice changes. *Science*, 278, 1104–1106.

Cheng, A. and R.H. Preller, 1996: The development of an ice-ocean coupled model in the Northern Hemisphere. *NRL/FR/7322-95-9627*, Naval Research Laboratory, Stennis Space Center, MS, 61 pp.

Cox, M., 1984: A primitive equation, 3-dimensional model of the ocean. *Geophysical Fluid Dynamics Laboratory Ocean Group Technical Report*, Princeton, NJ, 1141 pp.

Dukowicz, J.K. and R.D. Smith, 1994: Implicit free-surface method for the Bryan-Cox-Semtner ocean model. *J. Geophys. Res.*, 99(C4), 7991–8014.

Gow, A.J. and W.B.Tucker III, 1990: Sea ice in the polar regions. In: *Polar Oceanography Part A: Physical Science*. W.O. Smith Jr., Ed., Academic Press, NY, 47–122.

Hibler, W.D. III, 1979: A dynamic thermodynamic sea ice model. *J. Phys. Oceanogr.*, 9, 815–864.

Hibler, W.D. III, 1980: Modeling a variable thickness sea ice cover. *Monthly Weather Review*, 108, 1943–1973.

Hibler, W.D. III, 2000: On modeling the anisotropic failure and flow of flawed sea ice. *J. Geophys. Res.*, 105(C7), 17105–17120.

Hollinger, R.J., R. Lo, G. Poe, R. Savage and J. Pierce, 1991: *Special Sensor Microwave/Imager Calibration/ Validation—Final Report, Volume II*. Naval Research Laboratory, Washington, DC, 20 pp.

Jakobsson, M., N.Z. Cherkis, J. Woodward, R. Macnab and B. Coakley, 2000: A new grid of Arctic bathymetry: A significant resource for scientists and mapmakers. *EOS Transactions*, American Geophysical Union, 81(9), 89, 93, 96.

Johannessen, O.M., M. Miles and E. Bjorgo, 1995: The Arctic's shrinking sea ice. *Nature*, 376, 126–127.

Kwok, R., A. Schweiger, D. A. Rothrock, S. Pang and C. Kottmeier, 1998: Sea ice motion from satellite passive microwave imagery assessed with ERS SAR and buoy motions. *J. Geophys. Res.*, 103(C4), 8191–8214.

Levitus, S., 1982: Climatological Atlas of the World Ocean. *NOAA Prof. Pap.*, 13, 173 pp.

Maltrud, M.E., R.D. Smith, A.J. Semtner and R.C. Malone, 1998: Global eddy resolving ocean simulations driven by 1985–1995 atmospheric winds. *J. Geophys. Res.*, 103(C13), 30825–30853.

Maslowski, W., B. Newton, P. Schlosser, A. Semtner and D. Martinson, 2000: Modeling recent climate variability in the Arctic Ocean. *Geophys. Res. Lett.*, 27(22), 3743–3746.

Maslowski, W., D.C. Marble, W. Walczowski and A. Semtner, 2002: On large scale shifts in Arctic Ocean and sea-ice conditions during 1979-98. *Annals of Glaciology*, in press.

Meier, W.N., J.A. Maslanik and C.W. Fowler, 2000: Error analysis of remotely sensed ice motion within an Arctic sea ice model. *J. Geophys. Res.*, 105(C2), 3339–3356.

Naval Oceanographic Office (NAVOCEANO), 1997: D*atabase Description for Digital Bathymetric Data Base— Variable Resolution (DBDB-V,) Version 1.0.* Report, Naval Oceanographic Office, Stennis Space Center, MS.

National Geophysical Data Center, 1988: Digital relief of the Surface of the Earth. *Data Announcement 88-NGG-02*, NOAA National Geophysical Data Center Boulder CO.

Parkinson, C.L., D. Cavalieri, P. Gloersen, H.J. Zwally and J.C. Comiso, 1999: Arctic sea ice extents, areas and trends, 1978–1996. *J. Geophys. Res.*, 104, 20837–20856.

Parkinson, C.L. and W.M. Washington, 1979: A large-scale numerical model of sea ice. *J. Geophys. Res.*, 84, 311–337.

Preller, R.H. and P.G. Posey, 1995: Validation test report for a Navy sea ice forecast system: The Polar Ice Prediction System 2.0. *NRL/FR/7322-95-9634*, 31 pp.

Rigor, I.G. and A. Heiberg, 1997: I*nternational Arctic Buoy Program data report, 1 January 1995 √ 31 December 1995.* Applied Physics Laboratory, University of Washington, Seattle, Washington.

Sarmiento, J.L. and K. Bryan, 1982: An ocean transport model for the North Atlantic. *J. Geophys. Res.*, 87, 395–408.

Stark D.R., 2001: Response of a high resolution coupled ice/ocean model to the assimilation of ice motion fields derived from microwave satellite imagery. *Proceedings of the American Meteorology Society 6th Conference on Polar Meteorology and Oceanography*, May 14–18.

Steele, M., R. Morley and W. Ermold, 2001: Polar Science Center Hydrographic Climatology (PHC) A global ocean hydrography with a high quality Arctic Ocean. *J. Clim.*, 14, 2079–2087.

Van Woert, M.L., W.N. Meier, C.Z Zou, J.A. Beesley and P.D. Hovey, 2001: An assessment of the Polar Ice Prediction System ice concentration fields during May 2000. *Canadian Journal of Remote Sensin*g, in press.

Zhang, Y., W. Maslowski and A.J. Semtner, 1999: Impact of mesoscale ocean currents on sea ice in high-resolution Arctic ice and ocean simulations, *J. Geophys. Res.*, 104(C8), 18409–18429.